Dynamical topological quantum computation using spin pulse control in the Heisenberg model

Tetsufumi Tanamoto,[1] Keiji Ono,[2] Yu-xi Liu,[3,4,5] and Franco Nori[4,6]

[1] *Corporate R & D center, Toshiba Corporation, Saiwai-ku, Kawasaki 212-8582, Japan*
[2] *Low temperature physics laboratory, RIKEN, Wako-shi, Saitama 351-0198, Japan*
[3] *Institute of Microelectronics, Tsinghua University, Beijing 100084, China*
[4] *Center for Emergent Matter Science, RIKEN, Saitama 351-0198, Japan*
[5] *Tsinghua National Laboratory for Information Science and Technology (TNList), Beijing 100084, China*
[6] *Department of Physics, The University of Michigan, Ann Arbor, Michigan 48109-1040, USA*

(Dated: March 2, 2022)

Hamiltonian engineering is an important approach for quantum information processing, when appropriate materials do not exist in nature or are unstable. So far there is no stable material for the Kitaev spin Hamiltonian with anisotropic interactions on a honeycomb lattice (A. Kitaev, Annals of Physics **321** 2 (2006)), which plays a crucial role in the realization of both Abelian and non-Abelian anyons. Here, we show how to dynamically realize the Kitaev spin Hamiltonian from the conventional Heisenberg spin Hamiltonian using a pulse-control technique. By repeating the same pulse sequence, the quantum state is dynamically preserved. The effects of the spin-orbit interaction and the hyperfine interaction are also investigated.

PACS numbers: 03.67.Lx, 03.67.Mn, 73.21.La

Topological quantum computation (TQC) has attracted considerable interest due to its robustness to local perturbations [1]. Anyons, which obey different statistics from bosons and fermions, are also of fundamental interest in physics [2]. Kitaev [3] provided an important exactly-solvable model of a spin-1/2 system on a honeycomb lattice with potential links to topological quantum computation, for both Abelian and non-Abelian anyons. In the Kitaev honeycomb model, spin-spin interactions are realized by the so-called XX, YY, ZZ couplings along three directions (Fig. 1). This spin model stimulated the physics of an anyon system, including Majorana fermions. However, it is not easy to find materials which have such anisotropic interactions.

Even if we can find a possible material for realizing a desired Hamiltonian, we have to integrate and fabricate it by attaching many electrodes and probes to confirm whether it is sufficiently controllable. Regarding artificial realizations of the Kitaev Hamiltonian, theoretical proposals have been made using optical lattices [4, 5] and superconducting qubits [6]. In Ref.[6], You *et al.* used different qubit-qubit interactions depending on the coupling direction.

The Heisenberg model describes two-body interactions in many magnetic materials and artificial systems which are constructed by various fabrication techniques. In particular, quantum dot (QD) systems [7–12], donor systems [13–16], and nitrogen-vacancy (NV) centers [17–19] are promising candidates for spin-qubit systems, because they could be integrated on substrates by using advancing nanofabrication technology. The spin qubits in QDs also have the advantage that the tunneling coupling can be varied by attaching gate electrodes. Thus, placing QDs, with a single electron each, on a honeycomb lattice site is a promising way of realizing a Kitaev spin Hamiltonian.

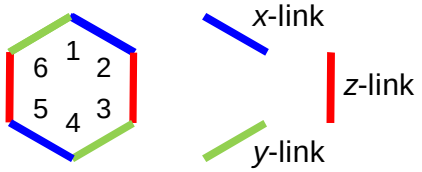

FIG. 1: (color online) Kitaev model on a honeycomb lattice.

Here we show how to dynamically generate this Hamiltonian starting from the natural Heisenberg model by using pulse-control techniques [20, 21]. Permanent data cannot be stored in quantum systems and should be transferred to attached conventional semiconductor memory, because the coherence time is less than a microsecond. From this point, it is natural to treat the qubit states dynamically with pulse control. Here, the Baker-Campbell-Hausdorf (BCH) formula is applied for producing a Kitaev Hamiltonian by taking into account the direction of the qubit-qubit couplings. Because unwanted terms are also generated in the BCH formula, the engineered Hamiltonian is effective for a finite time interval. Therefore, the dynamical approach requires a *refresh* process in which the same pulse sequence for generating the Kitaev Hamiltonian is carried out. The idea of repeating the production process is very common in conventional digital computers, such as dynamic random access memory (DRAM), which is a big capacitor and the amount of electric charge is lost over time [22].

Natural qubit-qubit interactions can be described by

either Ising, XY, or Heisenberg models. The most feasible one is the Ising interaction and the hardest one is the Heisenberg interaction [23]. It is not easy to transform the Heisenberg interaction to any desirable Hamiltonian because Heisenberg interactions have three components. Thus, the standard way to design Hamiltonians from the Heisenberg interaction is to change the Heisenberg interaction into an Ising interaction at the first step. Once we obtain the Ising interaction, we can transform it to a desirable interaction. However, as we will show, this method requires more than six steps to create a Kitaev Hamiltonian: three steps for obtaining XX,YY,ZZ interactions, plus additional three steps, for obtaining the corresponding x, y and z-links. What we would like to show here is that if we carefully design two-dimensional (2D) pulses which vary depending on qubit location, we can obtain the desired Hamiltonian in only one step. Because the topological Hamiltonian is derived from perturbation theory [3], we have to examine the direct effect of the unwanted terms, other than the spin-orbit (SO) terms and the hyperfine(HF) terms, on the topological Hamiltonian, focusing on the gapped phase (phase A).

Formulation.— The Kitaev Hamiltonian is given by the anisotropic spin model on the honeycomb lattice

$$H_K = -J_x \sum_{x-\text{links}} X_j X_k - J_y \sum_{y-\text{links}} Y_j Y_k - J_z \sum_{z-\text{links}} Z_j Z_k, \tag{1}$$

where X_j, Y_j and Z_j are the Pauli spin matrices and the interaction type (x, y, and z links) depends on the direction of the bond between the two sites (Fig. 1). The model in Eq.(1) can be mapped to free Majorana fermions coupled to a $\mathbb{Z}_2$ gauge field and have two types of interesting ground states (phase A and phase B) depending on the relative magnitude of J_x, J_y and J_z. The region $J_{\alpha_1} \leq J_{\alpha_2} + J_{\alpha_3}$, where α_i (i=1,2,3) refers to x,y,z, is the gapless B phase in which non Abelian anyons appear, and the other region is the gapped phase A, where Abelian anyon statistics is expected. In the B phase , an additional external magnetic field opens an energy gap.

We would like to derive Eq. (1) from the Heisenberg Hamiltonian given by

$$H_S = \sum_{i<j} [J_x X_i X_j + J_y Y_i Y_j + J_z Z_i Z_j]. \tag{2}$$

The "creation" of Eq. (1) is carried out by combining H_S with a transferred Hamiltonian H_R, which is produced by applying a customized pulse sequence to H_S, like NMR, using a repetition of the BCH formula. Concretely, the target Hamiltonian H_{tgt} is obtained by $H_{\text{tgt}} = H_S + H_R$, such as $e^{-itH_S} e^{-itH_R} \approx \exp(it[H_S + H_R] - t^2[H_S, H_R]/2 + ..)$, when $J_\alpha t \lesssim 1$. The terms higher than t are the unwanted ones $H^{\text{bch}}_{\text{uw}}$. As mentioned in the introduction, the standard way is to first create an Ising Hamiltonian and afterwards change the Ising Hamiltonian to a Kitaev Hamiltonian. We show that, if we consider the geometric distribution of the qubit on the honeycomb lattice, we can effectively create the Kitaev Hamiltonian.

Standard method.— The standard way to convert Eq. (2) to Eq. (1) requires six steps as shown in Fig. 2. The first step is to create the three Ising Hamiltonians, $H_x = \sum_{i,j} J_x X_i X_j$, $H_y = \sum_{i,j} J_y Y_i Y_j$, $H_z = \sum_{i,j} J_z Z_i Z_j$, from Eq. (2) as shown in Figs. 2(a,c,e). The generated Ising Hamiltonians are described by $H^\alpha_{\text{step1}} = \log[e^{itH_S} e^{itH^\alpha_{r1}}]/(it)$, where $H^\alpha_{r1} = P^{\alpha\dagger}_1 H_S P^\alpha_1$ ($\alpha = x, y, z$) is a rotated Hamiltonian by applying a $\pi/2$-pulse around the α-axes on the lattice sites of Figs. 2(a,c,e). The rotations consist of a multiple of the single rotations using formula $e^{-i(\pi/2)\sigma_\alpha} \sigma_\alpha e^{i(\pi/2)\sigma_\alpha} = -\sigma_\alpha$, for $X = \sigma_x$,$Y = \sigma_y$ and $Z = \sigma_z$. The next step is to erase unnecessary Ising interactions, such as $H^\alpha_{\text{step2}} = \log[e^{itH^\alpha_{\text{step1}}} e^{itH^\alpha_{r2}}]/(it)$, where $H^\alpha_{r2} = P^{\alpha\dagger}_2 H^\alpha_{\text{step1}} P^\alpha_2$ is obtained by applying $\pi/2$-pulses depending on the links in Figs. 2(b,d,f). Thus, the Kitaev Hamiltonian is dynamically obtained by $H^{\text{std}}_K(t) = \log[e^{itH^x_{\text{step2}}} e^{itH^y_{\text{step2}}} e^{itH^z_{\text{step2}}}]/(it)$. Note that parts of the Kitaev Hamiltonian do not commute, *i.e.* $[\sum_{x-\text{links}} X_j X_k, \sum_{y-\text{links}} Y_j Y_k] \neq 0$. Therefore, the unwanted terms increase in the standard method. A better method is presented below.

Efficient method.— The Kitaev Hamiltonian H_K is produced more efficiently from H_S when we apply rotation pulses more compactly. Figure 3 shows the distributions of the rotation pulses by which the BCH formula is used only once, such that $2\tau H^{\text{efc}}_K = \tau(H_S + H^{\text{efc}}_R)$. The x-link of the colored honeycomb is produced by applying a rotation around the y-axis and that around the z-axis on both sides of the link. Similarly, the y (z)-link is produced by a rotation around the z (x)-axis and around the x (y)-axis on both sides of the link.

If τ_{rot} denotes the time of a single-qubit rotation, it takes $2(2\tau_{\text{rot}} + \tau)$ and $12(2\tau_{\text{rot}} + \tau)$ to create rotations $\exp(-i2\tau H^{\text{efc}}_K)$, and $\exp(-i4\tau H^{\text{std}}_K)$, respectively. Similarly to the conventional DRAM, when we define *refresh overhead* as the effectiveness of the refresh of the quantum state such as

$$\text{refresh overhead} = \frac{\text{time required for refresh}}{\text{refresh interval}}. \tag{3}$$

The refresh overhead of the efficient method presented above is $(2\tau_{\text{rot}} + \tau)/\tau \approx 2J_z\tau_{\text{rot}} + 1$, and that of the standard method shown previously is $3(2J_z\tau_{\text{rot}} + 1)$, for $J_z\tau \lesssim 1$. Thus, the efficient method is three times efficient than the standard method.

Fidelity.— Let us numerically estimate the improvement of the efficient method by calculating a *gate fidelity* [24]. The time-dependent gate fidelity is defined by

$$F(t) = |\text{Tr}[\exp[itH_K] U_{\text{P}}(t)]|/2^N, \tag{4}$$

where $U_{\text{P}}(t)$ denotes the evolution operator of the pulsed system. The gate fidelity shows how well

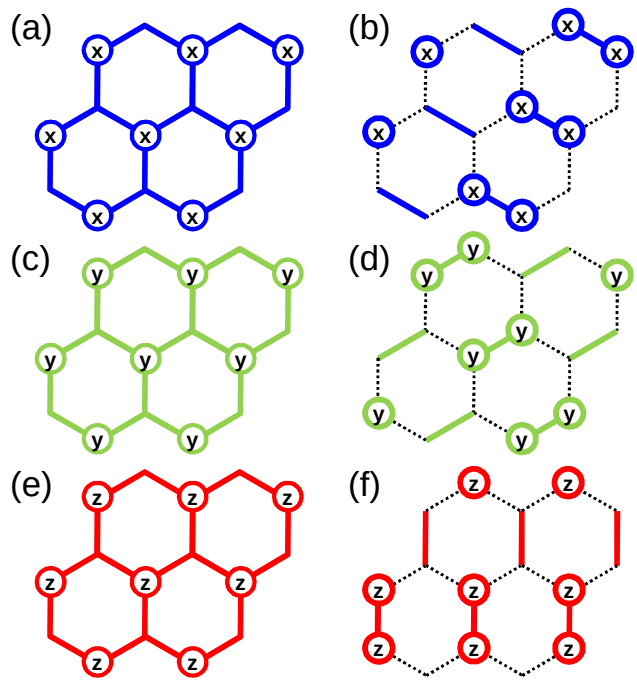

FIG. 2: (color online) Standard method to dynamically produce a Kitaev Hamiltonian from the Heisenberg model. The symbols x, y and z in the lattice sites show the application of $\pi/2$-pulses around x, y and z, respectively. The bonds with dotted lines indicate that there is no interaction between the connected sites. (a) Pulse mapping of P_1^x to create the Ising Hamiltonian, $H^x_{\rm step1} = \sum_{i,j} J_x X_i X_j$ in $e^{itH^x_{\rm step1}} = e^{itH_S} e^{itP_1^{x\dagger} H_S P_1^x}$. (b) Pulse mapping to select only the x-link of the Kitaev Hamiltonian from the Ising Hamiltonian of (a). (c) and (e) express pulse distributions for generating $H_y = \sum_{i,j} J_y Y_i Y_j$ and $H_z = \sum_{i,j} J_z Z_i Z_j$, respectively. (d) and (f) show pulse the pattern to select only the y and z links, respectively.

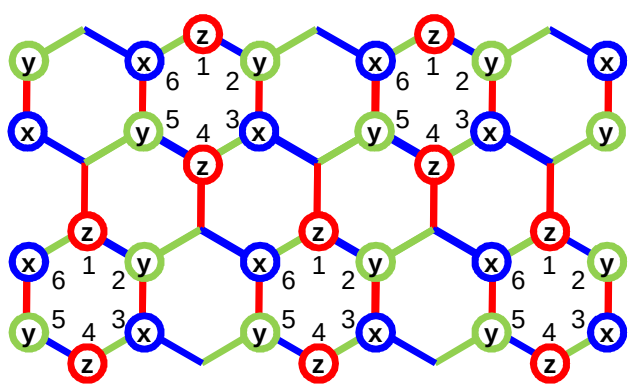

FIG. 3: (color online) The *efficient* pulse distribution $P_{\rm efc}$ for $H_R^{\rm efc} = P_{\rm efc}^\dagger H_S P_{\rm efc}$ in order to dynamically produce a Kitaev Hamiltonian from the Heisenberg model via one step. The x, y and z on the lattice sites show the application of $\pi/2$-pulses around x, y and z, respectively.

the transformed Hamiltonian evolves compared with H_K. For the standard arrangement, $U_{\rm P}(t)$ is given by $U_{\rm P}(t) = U_{\rm x}^{(1)}(t)U_{\rm x}^{(2)}(t)U_{\rm y}^{(1)}(t)U_{\rm y}^{(2)}(t)U_{\rm z}^{(1)}(t)U_{\rm z}^{(2)}(t)$, with $U_\alpha^{(i)}(t) = \exp[-itH_S]R_\alpha^{(i)}\exp[-itH_S]R_\alpha^{(i)}$, for $i = 1, 2$ and $\alpha = x, y, z$. $R_\alpha^{(1)}$ and $R_\alpha^{(2)}$ transform H_S into the rotated ones shown in Figs. 2(a,c,e) and (b,d,f), respectively. In contrast to this, for the efficient pulse arrangement, $U_{\rm P}(t)$ is simply expressed by $U_{\rm P}(t) = \exp[-itH_S]\exp[-itH_R]$.

Here the SO interaction and the HF interaction are included. The SO interaction is expressed by $V_{\rm so} = \sum_{jk}[\mathbf{c}_{\rm so}\cdot(\boldsymbol{\sigma}_j - \boldsymbol{\sigma}_k) + \mathbf{d}_{\rm so}\cdot\boldsymbol{\sigma}_j\times\boldsymbol{\sigma}_k]$, where $\boldsymbol{\sigma}_j = (X_j, Y_j, Z_j)$, and the magnitudes of the spin-orbit vectors $\mathbf{c}_{\rm so} = (c_x, c_y, c_z)$ and $\mathbf{d}_{\rm so} = (d_x, d_y, d_z)$ are 10^{-2} smaller than J_z [25]. The HF interaction is given by the fluctuation of the field such as $V_{\rm hp} = -\sum_j(\delta h_x X_j + \delta h_y Y_j + \delta h_z Z_j)$ [26]. We treat the hyperfine field as a static quantity because the evolution of the hyperfine field is $\sim$10 μs and slower than the time scale of the pulse control $\sim$ 100 ns [9]. The total Hamiltonian of this system in the calculation is expressed by $H = H_S + V_{\rm so} + V_{\rm hp}$. The Chebyshev expansion method is used for calculating the time-dependent behavior until its 6th-order term [27]. Figure 4 shows the numerical results for $N = 10$ qubits (two honeycomb lattices). The calculations include several cases for different parameters (i) $J_x = J_y = 0.3J_z$, $d_\alpha = 0$, and $\delta h_\alpha = 0$, (ii) $J_x = J_y = 0.3J_z$, $d_\alpha = 0.1$, and $\delta h_\alpha = 0.1$, and (iii) $J_x = J_y = J_z$, $d_\alpha = 0.3$, and $\delta h_\alpha = 0.3$ ($\alpha = x, y, z$). In various parameter regions, the overlap with the Kitaev Hamiltonian by using the pulse-controlled method is excellent. We can also find that the repetition of the BCH formula [21] greatly increases the gate fidelity. In Fig. 4, 'BCH–2' means that two identical BCH operations are repeated in a given time t (See also Sec.I of [30]). The repetition of the same operation also leads to the bang-bang control and reduces the effect of the noisy environment [28]. The same feature is confirmed for a single honeycomb lattice ($N = 6$). Thus we can say that the dynamical method on the Heisenberg model can realize the Kitaev Hamiltonian.

In order to directly see the effects of the unwanted terms, SO terms, and HF terms, we calculate the time-dependent eigenvalues of the effective Hamiltonian $H_{\rm eff} = \{H_S + H_R - i(t/2)[H_S, H_R]\}/2$, as shown in Fig. 3. Because of limited computational resources, we show the numerical results for $N = 6$ and $N = 10$. We can find that an energy gap opens up in the $J_z t \lesssim 1$ region. The energy gap becomes narrow for $N = 10$, compared for $N = 6$, because of finite-size effects. When we compare Fig. 5(d) with Fig. 5(c), we find that the SO terms and the HF terms decrease the energy gap for large-N systems.

Toric code Hamiltonian.— The unperturbed Hamiltonian of the A phase is given by $H_0 = -J_z\sum_{z-\rm links} Z_j Z_k$, whose ground state is a degenerate dimer state. The

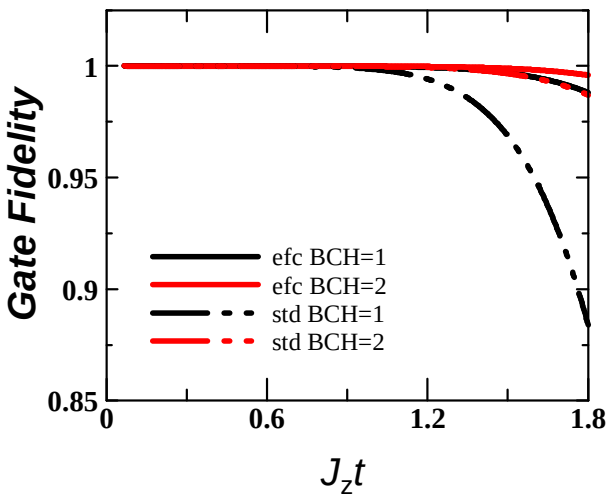

FIG. 4: (color online) Numerically calculated gate fidelity. Here "std" corresponds to the *standard* method (Fig. 2), and "efc" corresponds to the *efficient* method (Fig. 3), respectively. "BCH–n" means that the BCH formula is applied n times. Repeating the BCH formula corresponds to a *refresh*

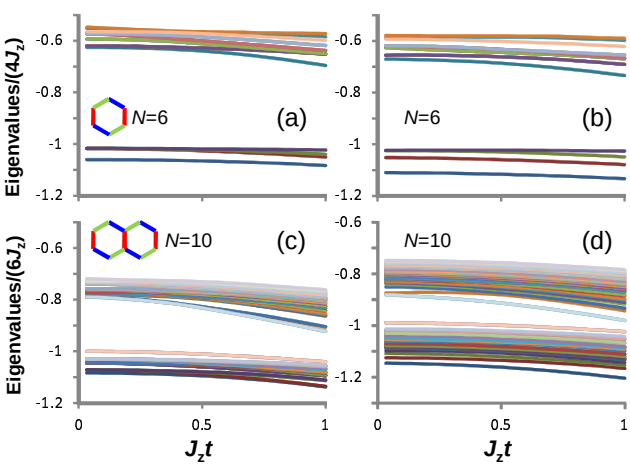

FIG. 5: (color online) Time-dependent eigenvalues of the effective Hamiltonian $H_{\rm eff} = \{H_S + H_R - i(t/2)[H_S, H_R]\}/2$ for $N = 6$ (a,b) and $N = 10$ (c,d). $J_x = J_y = 0.3J_z$ (a,c) use $d_x = d_y = \delta h_x = \delta h_y = 0$. (b,d) use $d_x = d_y = \delta h_x = \delta h_y = 0.1J_z$. Eigenenergies are scaled by J_z.

Hamiltonian in the dimer state can be expressed by "effective spin operators", X^e, Y^e and Z^e, by pairing original spin operators, such as $P[X \times Y] \to Y^e$, $P[X \times X] \to X^e$, $P[Y \times Y] \to -X^e$, $P[Z \times I] \to Z^e$, and $P[Z \times Z] \to I^e$ [29]. These pairs are taken between sites 2-3 and 5-6 in Fig. 1. The spins of the sites 1 and 4 are paired with the spins of another honeycomb lattice. Then $V_0 = -J_x \sum_{x-\rm links} X_j X_k - J_y \sum_{y-\rm links} Y_j Y_k$ acts as a perturbation and generates an effective Hamiltonian $H^K_{\rm eff} = -J^K_{\rm eff} \sum_p Q_p$, with $J^K_{\rm eff} = (J_x^2 J_y^2/16J_z^3)$ and $Q_p = Y^e_{p,4} Y^e_{p,2} Z^e_{p,1} Z^e_{p,4}$ in their forth-order effects. Therefore, here we have to compare $H^K_{\rm eff}$ with the perturbation terms in the BCH formula, the SO interaction, and the HF interaction in the same framework as the Kitaev perturbation theory. It is obvious that the smaller magnitude of the SO terms and the HF interactions are desirable to achieve the condition that $J_z > \{J_x, J_y, |\vec{h}|\} > \{|\delta\vec{h}_{\rm hf}|, c_{\rm so}, d_{\rm so}\}$. Here we show that we have more constraints to realize the TQC. We also consider the commutation relation with a *plaquette operator* given by $W_p = Z_1 Y_2 X_3 Z_4 Y_5 X_6$, where W_p commutes with the Hamiltonian Eq. (1), and is described by $W^e_p = Z^e_1 Y^e_2 Z^e_3 Y^e_4$.

Let us start with the first-order unwanted terms in the BCH formula, given by $H_{\rm uw} = -it[H_S, H_R]/4$. Many terms appear from this commutations relations (see Sec.IV of Ref. [30]). In order to see their typical effect, here we choose the unwanted terms that originate from the single honeycomb whose six qubits are rotated (the center-bottom honeycomb in Fig. 3). These terms are explicitly expressed such as

$$H^{(l;z,x)}_{\rm uw} = (t_0/n) J_z J_x [Y_l X_{l+1} Z_{l+2} - X_l Z_{l+1} Y_{l+2}], \quad (5)$$
$$H^{(l+1;y,z)}_{\rm uw} = (t_0/n) J_z J_y [X_{l+1} Z_{l+2} Y_{l+3} - Z_{l+1} Y_{l+2} X_{l+3}], \quad (6)$$
$$H^{(l+2;x,y)}_{\rm uw} = (t_0/n) J_x J_y [Z_{l+2} Y_{l+3} X_{l+4} - Y_{l+2} X_{l+3} Z_{l+4}], \quad (7)$$

for $l = 1, 4$. Because these terms do not commute with W_p nor the Hamiltonian Eq.(1), they are unwanted terms in the topological quantum computation. The effective Hamiltonian of Eqs.(5)-(7) appears in the second-order perturbation given by $\langle a|H^{(2)}_{\rm eff}|b\rangle = \sum'_j [\langle a|V|j\rangle\langle j|V|b\rangle/(E_0 - E_j)]$, which is expressed as

$$\begin{aligned} H^{\rm uw}_{\rm eff} \approx t^2 \{ & J_z \left[J_x^2 (X^e_1 X^e_2 + X^e_3 X^e_4) + J_y^2 (X^e_2 X^e_3 + X^e_4 X^e_1) \right] \\ + \quad & J_x^2 J_y (2 Z^e_2 Z^e_4 - Z^e_1 X^e_2 Z^e_4 - Z^e_3 Z^e_2 X^e_4) \\ + \quad & J_x J_y^2 (2 Z^e_2 Z^e_4 + Z^e_1 Z^e_2 X^e_4 + Z^e_3 X^e_2 Z^e_4) \}. \end{aligned} \quad (8)$$

Thus, this term commutes neither with the Kitaev Hamiltonian nor with W_p. From this approximation, to realize a TQC, we have a constraint on the time, given by $t^2 J_\alpha^2 J_z < J^K_{\rm eff}$. When $J_x = J_y$, this corresponds to $t < J_x/(4J_z^2)$. The effective SO terms are derived in the similar manner. There are many terms regarding the SO interactions (See Sec.VI of Ref. [30]), all of which do not commute with W_p nor the Hamiltonian Eq.(1). As an example, the effective SO terms of the center honeycomb lattice at the bottom row in Fig. 3 are given by $H^{\rm so}_{\rm eff} = [2d_x d_y (X^e_2 + X^e_4)/J_z]$. The effect of the HF interaction is expressed by $H^{\rm hp}_{\rm eff} = [\langle \delta h_{x2} \delta h_{y3} \rangle Y^e_2 + \langle \delta h_{x5} \delta h_{y6} \rangle Y^e_4]/J_z$, assuming the uniformity of the HF interaction, such as $\langle \delta h_{x2} \delta h_{x3} \rangle = \langle \delta h_{y2} \delta h_{y3} \rangle$. This term also does not commute with W_p nor the Hamiltonian Eq.(1). From these estimates, in order to realize the TQC, both the SO and the HF interactions should be small and we have the constraint $2d_x d_y/J_z$ and $\langle \delta h_{x5} \delta h_{y6} \rangle / J_z < J^K_{\rm eff}$.

Discussion.— Let us consider a process of TQC in spin qubits. The toric code and the surface code are based on stabilizer formalism [31, 32], where desired quantum states are obtained by stabilizer measurements. These measurements can be carried out by conventional spin-qubit operations by manipulating the Heisenberg model with appropriate magnetic fields. However, because the desired states are not always eigenstates of the Heisenberg Hamiltonian, the desired states are not preserved. Thus, the present method which can preserve the desired states of the TQC is important after the measurement. Let us estimate the measurement time from this scheme. In each measurement process of the surface code, four CNOT gates and two Hadamard gates are required [31]. When each CNOT gate consists of two $\sqrt{\text{SWAP}}$s [8] and each $\sqrt{\text{SWAP}}$ requires a time $\pi/(8J_{\text{meas}})$, where J_{meas} is a Heisenberg coupling strength for the measurement, one stabilizer measurement cycle approximately requires a time π/J_{meas}. Because a short measurement time and a long coherence-preserving time ($\sim J_z^{-1}$) are preferable, it is desirable for the coupling strength between qubits to be changeable, therefore $J_{\text{meas}} > J_z$ is desirable.

In spin-qubit systems based on QDs, the coupling J_{jk} exponentially changes as the distance between two QDs or the gate voltage changes [9–11]. As an example, $J \approx 0.1$–1 μeV is obtained, when the voltage difference between two GaAs QDs is less than 10 mV [9], and we can choose $J_z \approx 0.1$ μeV and $J_{\text{meas}} \approx 1$ μeV. When $J_z \approx 0.1$ μeV ($= 0.0116$ K), the period $J_z t \lesssim 1$ corresponds to $t \sim 24.2$ ns. In the typical DRAM array, every row is refreshed about every 15 μs [22]. Thus, compared with the conventional DRAM, a more frequent refresh is required in our proposal.

Experimentally, spin-qubit systems are realized by either Si donors or NV centers, in addition to semiconductor QDs, such as GaA or SiGe. The SO and the HF interactions are strongest in GaAs systems and smallest in donor systems and NV centers. The controllability of spins is better for GaAs systems and difficult in donor systems and NV centers. Thus there is a tradeoff between the controllability and the realization of TQC.

In summary, we proposed how to dynamically generate a Kitaev spin Hamiltonian on a honeycomb lattice from the Heisenberg spin Hamiltonian by using a dynamical average Hamiltonian theory. We also considered the effects of the unwanted terms of the BCH, SO interaction, and HF interactions. We clarified that if these terms are sufficiently small, a dynamic TQC is available by periodically reproducing the topological Hamiltonian.

TT would like to thank A. Nishiyama, K. Muraoka, S. Fujita, and H. Goto for discussions. YXL is supported by the National Natural Science Foundation of China under Grant Nos. 61025022, 91321208, the National Basic Research Program of China Grant No. 2014CB921401. FN is partially supported by the RIKEN iTHES Project, MURI Center for Dynamic Magneto-Optics, and a Grant-in-Aid for Scientific Research (S).

[1] X.G. Wen, *Quantum Field Theory of Many-body Systems* (Oxford University Press, New York, 2004).
[2] F. Wilczek, *Fractional Statistics and Anyon Superconductivity* (World Scientific, Singapore, 1990).
[3] A. Kitaev, Annals of Physics **321**, 2 (2006).
[4] L.M. Duan, E. Demler, and M.D. Lukin, Phys. Rev. Lett. **91**, 090402 (2003).
[5] M. Aguado, G.K. Brennen, F. Verstraete, and J.I. Cirac, Phys. Rev. Lett. **101**, 260501 (2008)
[6] J.Q. You, X.F. Shi, X. Hu, and F. Nori, Phys. Rev. B **81**, 014505 (2010).
[7] D. Loss and D.P. DiVincenzo, Phys. Rev. A **57**, 120 (1998).
[8] G. Burkard, D. Loss, D.P. DiVincenzo, and J.A. Smolin, Phys. Rev. B **60**, 11404 (1999).
[9] J.R. Petta, A. C. Johnson, J. M. Taylor, E. A. Laird, A.Yacoby, M. D. Lukin, C. M. Marcus, M. P. Hanson, A. C. Gossard, Science **309**, 2180 (2005).
[10] G. Burkard, G. Seelig, and D. Loss, Phys. Rev. B **57**, 2581 (2000).
[11] X. Hu and S. Das Sarma, Phys. Rev. A **61** 062301 (2000).
[12] K. Ono D.G. Austing and Y. Tokura, Science **297**, 1313 (2002).
[13] B.E. Kane, Nature (London) **393**, 133 (1998).
[14] J. Salfi, J. A. Mol, R. Rahman, G. Klimeck, M.Y. Simmons, L.C L. Hollenberg and S. Rogge, Nature Materials, **13**, 605 (2014).
[15] E. Hamid, D. Moraru, Y. Kuzuya, T. Mizuno, L. T. Anh, H. Mizuta, and M. Tabe Phys. Rev. B **87**, 085420 (2013).
[16] K. Ono, T. Tanamoto and T. Oguro, Appl. Phys. Lett. **103**, 183107 (2013).
[17] F. Jelezko, T. Gaebel, I. Popa, A. Gruber, and J. Wrachtrup Phys. Rev. Lett. **92**, 076401 (2004).
[18] N.Y. Yao, L. Jiang, A.V. Gorshkov, Z.-X. Gong, A. Zhai, L.-M. Duan, and M.D. Lukin, Phys. Rev. Lett. **106**, 040505 (2011).
[19] Y. Ping, B.W. Lovett, S.C. Benjamin, and E. M. Gauger, Phys. Rev. Lett. **110**, 100503 (2013).
[20] R.R. Ernst, G. Bodenhausen, and A. Wokaun, *Principles of Nuclear Magnetic Resonance in One and Two Dimensions* (Oxford University Press, Oxford, 1987).
[21] T. Tanamoto, Phys. Rev. A **88**, 062334 (2013).
[22] B. Keeth and R.J. Baker, *DRAM Circuit Design: A Tutorial* (John Wiley & Sons, 2001).
[23] T. Tanamoto, Y.X. Liu, X. Hu and F. Nori, Phys. Rev. Lett. **102**, 100501 (2009).
[24] D. Becker, T. Tanamoto, A. Hutter, F.L. Pedrocchi, and D. Loss Phys. Rev. A **87**, 042340 (2013).
[25] F. Baruffa, P. Stano, and J. Fabian Phys. Rev. B **82**, 045311 (2010).
[26] L. Cywinski, Acta Phys. Pol. A **119**, 576 (2011).
[27] R. Kosloff and H. Tal-Ezer, Chem. Phys. Lett. **127**, 223 (1986).
[28] L. Viola and S. Lloyd, Phys. Rev. A **58**, 2733 (1998).
[29] G. Kells, A.T. Bolukbasi, V. Lahtinen, J.K. Slingerland, J.K. Pachos, and J. Vala Phys. Rev. Lett. **101** 240404 (2008).
[30] To be published elsewhere.

[31] A.G. Fowler, M. Mariantoni, J.M. Martinis, and A.N. Cleland, Phys. Rev. A **86**, 032324 (2012).

[32] S.B. Bravyi, A.Yu. Kitaev, quant-ph/9811052.